

Cyclotron resonance of high-mobility two-dimensional electrons at extremely low densities

M. J. Chou and D. C. Tsui

Department of Electrical Engineering, Princeton University, Princeton, New Jersey 08544

G. Weimann

Forschungsinstitut der Deutschen Bundespost, Postfach 5000, D-6100 Darmstadt, Germany

(Received 30 June 1987)

We have systematically studied the cyclotron resonance (CR) of high-mobility two-dimensional electrons in GaAs/Al_xGa_{1-x}As heterostructures at $T=4.2$ and 2.3 K in low densities ranging from $n_s=1.55\times 10^{10}$ to 1.03×10^{11} cm⁻², in the extreme quantum limit from filling factor $\nu\approx 0.6$ to $\nu\approx 0.08$. For $0.4 < \nu < 0.6$, the effect of level crossing dominates the CR and its linewidth. The effective mass, after nonparabolicity correction, is constant to better than 0.025% from $\nu=0.4$ to 0.14 and decreases by $\Delta m_0^* \approx 7\times 10^{-4}m_0$ from $\nu=0.14$ to 0.08. The CR lifetime τ_{CR} is 104 ps at $\nu=0.4$, which is 15 times the dc scattering time and the longest CR lifetime reported. In the range $0.08 < \nu < 0.4$ the dependence of τ_{CR} on n_s follows a power law, $\tau_{\text{CR}} \propto n_s^{1.9\pm 0.1}$. We attribute this n_s -dependent τ_{CR} in the extreme quantum limit to scattering by screened residual ionized impurities in GaAs. Our studies also resolve the existing experimental discrepancies concerning the oscillatory behavior of the CR linewidth as a function of ν .

I. INTRODUCTION

Cyclotron resonance (CR) of two-dimensional electron gas (2D EG) has attracted numerous experimental¹⁻¹⁹ and theoretical²⁰⁻³⁰ investigations since it was first observed in the inversion layer at the Si-SiO₂ interface.^{1,2} Of particular current interest is the CR in the low-density (n_s) and high-magnetic-field (B) limit when only the lowest Landau level is partially filled. In this extreme quantum limit, electron correlation can be dominant and the 2D EG is expected to crystalize into a Wigner solid.³¹ To date, such a Wigner crystal remains elusive. The fractional quantum Hall effect,³² recently discovered in an experimental search for the Wigner crystal, is the manifestation of a series of novel fluid states,³³ which may be regarded as a precursor to the crystalline state.

The n_s in the Si-SiO₂ system can in principle be changed from zero to 10^{13} cm⁻², limited only by the breakdown field of SiO₂. In practice, however, owing to the strong interfacial potential fluctuations,³⁴ the minimum n_s available is $\sim 10^{11}$ cm⁻². The GaAs/Al_xGa_{1-x}As heterostructure, on the other hand, is made of lattice-matched single crystals and is known to have better interface properties. The use of selective-doping techniques³⁵ has improved the interface to such exceptional perfection that μ_{dc} , the dc mobility of the 2D EG, of $\sim 5\times 10^6$ cm²/V sec at 4.2 K has been reported recently.³⁶ The n_s of the 2D EG is given by the doping level of Si impurities in the Al_xGa_{1-x}As and by the thickness of the undoped Al_xGa_{1-x}As spacer layer of the structure. In addition, n_s can also be changed by the application of a gate voltage or by illumination with light.³⁷ The maximum and minimum n_s that have been reported are 1.1×10^{12} and 3.5×10^{10} cm⁻², respectively.^{37,7}

In principle, CR gives directly the effective mass from the magnetic field position B_{CR} of the resonance, and the scattering rate from the resonance linewidth. In practice, however, the observations are seldom free of interesting complications. More specifically, Englert *et al.*⁸ first studied the CR in low-density samples and found that the linewidth oscillates as a function of the Landau-level filling factor ν , which is defined by $\nu=2\pi l_0^2 n_s$ and the cyclotron radius of the lowest Landau level $l_0=\sqrt{\hbar/eB}$. Their observation, made on samples with $n_s \leq 2.5\times 10^{11}$ cm⁻² and $\mu_{\text{dc}} \sim 100\,000$ cm²/V sec, is attributed to the dependence of impurity screening on the occupation of Landau levels and has inspired much theoretical discussion.²⁵⁻²⁸ It has also encountered serious discrepancies from subsequent experiments. In particular, such oscillatory behavior in linewidth has not been observed in high-density samples. Moreover, Muro *et al.*¹² used a front gate to reduce the n_s and observed CR down to $n_s=5.5\times 10^{10}$ cm⁻². Their CR linewidth increases monotonically with decreasing n_s , showing no dependence on ν . More recently, Schlesinger *et al.*⁹ studied the CR in the extremely quantum limit with $n_s \geq 3.5\times 10^{10}$ cm⁻². They observed broadening, as well as a line shift at $\nu\sim 1$, which they attributed to electron-electron interactions.

In this paper we report our investigation of CR of a high-mobility 2D EG in the GaAs/Al_{0.35}Ga_{0.65}As heterostructure in the low-density range from $n_s=1.03\times 10^{11}$ to 1.55×10^{10} cm⁻² with $\mu_{\text{dc}}=300\,000$ cm²/V sec at $n_s=1.0\times 10^{11}$ cm⁻². The experiment was carried out at $T=4.2$ and 2.3 K, using a far-infrared (FIR) laser with $\lambda=96.52$ μm . The cyclotron energy ($\hbar\omega_c=12.85$ meV) is larger than the Coulomb energy ($E_c=e^2/4\pi\epsilon\epsilon_0 l_0 \approx 11.9$ meV),³⁰ but still smaller than the LO-phonon energy (~ 36 meV).¹¹ This arrangement en-

ables us to focus on the narrow linewidth of the resonance and study the effect of level filling in the extreme quantum limit from $\nu \simeq 0.6$ to $\nu \simeq 0.08$.

We found that the CR shows a Lorentzian line shape and that the linewidth is extremely narrow and strongly dependent on ν . The half-width at half maximum (HWHM) varies from $\Delta B = 0.6$ to 0.012 T. In the range $0.4 < \nu < 0.6$, the linewidth is due to the subband level-crossing effect previously observed by Schlesinger *et al.*¹⁵ At $\nu \sim 0.4$, the CR lifetime τ_{CR} , extracted from the data by fitting the entire CR curve, is 104 ps, which is 15 times the dc scattering time and the longest ever reported. As n_s decreases and ν decreases from $\nu \simeq 0.4$ to $\nu \simeq 0.08$, the dependence of τ_{CR} on n_s follows $\tau_{\text{CR}} \propto n_s^{1.9 \pm 0.1}$. We attribute this n_s -dependent lifetime in the extreme quantum limit to scattering by screened residual ionized impurities in GaAs. The cyclotron mass, on the other hand, can be determined directly from the CR position to extremely high relative accuracy. The effective mass m_c^* , after the nonparabolicity correction, is constant to better than 0.025% from $\nu \simeq 0.4$ to $\nu \simeq 0.14$. For $0.4 < \nu < 0.6$, variations in mass due to the subband level crossing are observed. From $\nu \simeq 0.14$ to $\nu \simeq 0.08$, m_c^* decreases by $\Delta m_c^* \simeq 7 \times 10^{-4} m_0$. This small shift may be indicative of localization at extremely low n_s due to either potential fluctuations or the electron correlation. We have also extended our measurements to $T = 2.3$ K and examined the CR position and the linewidth. We found no structure at $\nu = \frac{1}{3}$ and $\frac{1}{5}$, where the fractional quantum Hall effect is known to exist, and we also found no structure at $\nu = \frac{1}{11}$.

Our experiment also makes clear the origin of the discrepancies concerning the oscillatory behavior of the CR linewidth as a function of ν for $\nu > 1$. The fact that such oscillatory behavior has not been observed in high n_s samples is understood in terms of the saturation effect, which we shall discuss in more detail in Sec. III. The data of Muro *et al.*¹² can be explained by the inhomogeneity in n_s induced by the front gate voltage. Since the CR position, due to nonparabolicity, is n_s dependent, the inhomogeneity induced by the front gate increases the linewidth. We have observed this effect and the results from these front gate measurements are discussed in detail in another publication.³⁸

II. EXPERIMENTAL DETAILS

The samples used in this work are from a wafer of selectively doped GaAs/Al_{0.35}Ga_{0.65}As heterostructure with a 3- μm -thick buffer layer. The Si donors were placed 910 Å away from the GaAs/Al_xGa_{1-x}As interface. This large setback reduces the strength of the surface fluctuations at the interface and results in a low- n_s and high-mobility 2D EG. In order to have a wide range of carrier density, a back gate voltage is used in this work to change n_s capacitively. The substrate was first polished mechanically, using 5- μm SiC particles. Subsequently, the chemical polishing, using 0.3% bromine in methanol, was carried out to give the final thickness of ~ 90 μm with an unintentionally wedged angle

$\sim 0.6^\circ$. Ohmic contacts were made at the four corners of the sample by alloying indium in a hydrogen ambient at 400°C for 20 min after the sample was cleaned thoroughly in organic solvents. A 150-Å semitransparent titanium layer was then evaporated on the polished surface of the substrate as the back gate. The sample was mounted on a copper piece, which has a hole of $\frac{3}{32}$ in. in diameter, with Apiezon grease, and the back-gate voltage was applied to the copper with respect to the Ohmic contacts on the sample. A piece of black polyethylene blocking the blackbody radiation and a linear polarizer were placed before the sample for FIR transmission measurements.

In this experiment, the gate voltage V_g is operated in the range $-150 \leq V_g \leq +150$ V, limited by the leakage current. In the range $0 \leq V_g \leq +150$ V, the densities, determined by the Shubnikov-de Haas (SdH) oscillations, depend linearly on V_g following

$$n_s = (5.9 + 0.029V_g) \times 10^{10} \text{ cm}^{-2}. \quad (1)$$

For negative bias, $-150 \leq V_g < 0$ V, the n_s , too low to allow SdH measurements, is estimated using Eq. (1). We obtained a density range $1.55 \times 10^{10} \leq n_s \leq 1.03 \times 10^{11} \text{ cm}^{-2}$, corresponding to a Fermi energies $0.55 \leq E_f \leq 3.7$ meV. The dc mobility μ_{dc} , obtained by the van der Pauw method, increases with increasing n_s following a power law $\mu_{\text{dc}} \propto n_s^{1.6}$ for $n_s \geq 6.77 \times 10^{10} \text{ cm}^{-2}$ (with $\mu_{\text{dc}} = 1.65 \times 10^5 \text{ cm}^2/\text{V sec}$ at $n_s = 6.77 \times 10^{10} \text{ cm}^{-2}$). This result implies that ionized impurity scattering is the dominant scattering mechanism.^{39,40} For lower densities, the inhomogeneity causes strong fluctuations in the dc conductivity and makes the determination of μ_{dc} impossible.

The CR experiments were performed by using the swept-field method under the Faraday configuration, as discussed in Ref. 14. The magnetic field is provided by a superconducting magnet, and the far-infrared radiation is generated by an optically pumped FIR laser. A laser wavelength of 96.52 μm , corresponding to a photon energy $\hbar\omega$ of 12.85 meV, was chosen to avoid interference effects. This choice has also made it possible to realize the extreme quantum limit, $0.085 \leq \nu \leq 0.56$, with the available n_s . As a result, the cyclotron radius of the electrons is $l_0 = 94$ Å, smaller than the average interelectron separation, $1/(\pi n_s)^{1/2}$. The experiments were carried out at $T = 4.2$ and 2.3 K under a constant FIR intensity of ~ 1 mW/cm².

III. DATA AND ANALYSES

The solid curves in Fig. 1 show five typical traces of the CR data at $T = 4.2$ K for $V_g = 30, 0, -50, -100,$ and -150 V, where $T(B)$ and $T(0)$ are the transmittance with and without B , respectively. Three observations are worth emphasizing. First, the CR width is extremely narrow, indicating that the CR mobility is very high in these low n_s regimes. For example, the HWHM is 0.0122 ± 0.0005 T for $V_g = 30$ V. It increases to 0.027 ± 0.001 T at $V_g = -150$ V. Second, the resonance amplitude is large, a consequence of the narrow width.

For $V_g = 30$ V, it corresponds to a 45.5% change in transmittance, and it decreases monotonically to 3.3% at $V_g = -150$ V. This makes the total absorption area decrease as V_g is more negatively biased, consistent with the fact that n_s is decreased. Third, B_{CR} is higher than that of bulk GaAs, which is expected at 7.38 T. For example, $B_{CR} = 7.64$ T for $V_g = 30$ V and it shifts to even higher field as V_g is negatively biased. For $V_g = -150$ V, B_{CR} is 7.66 T, corresponding to a 0.25% increase from that for $V_g = 30$ V.

Since the resonance is sharp, the B_{CR} can be identified unambiguously with a reproducibility of ± 0.001 T. The effective mass m_{CR}^* , obtained directly from B_{CR} through $m_{CR}^* = eB_{CR}/\omega$, is plotted against V_g and n_s in Fig. 2, and the corresponding ν is marked in the top frame. The m_{CR}^* decreases monotonically from $0.06903m_0$ to $0.06882m_0$ as n_s is increased, and has a faster decrease near $n_s \sim 9 \times 10^{10} \text{ cm}^{-2}$, which is close to $\nu \sim 0.5$.

In order to extract τ_{CR} or μ_{CR} (the CR mobility) from our data, we use the Drude model and calculate the complex dielectric function and the transmittance. The transmission coefficient t_{\pm} and the measured transmittance $T(B)$, obtained from the matrix method presented in Ref. 14, can be expressed as follows:

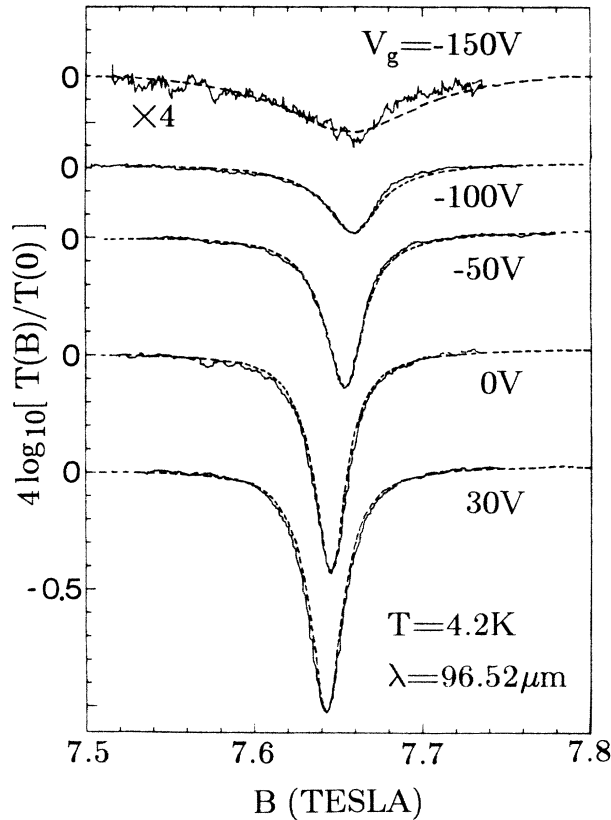


FIG. 1. Solid curves: experimental traces of cyclotron resonance as a function of B for different back-gate voltage. Dashed curves: fits of the transmittance to Eq. (2) using τ_{CR} as the fitting parameter. The corresponding τ_{CR} from top to bottom curves are 7.7, 19, 42, 73, and 104 ps, respectively.

$$t_{\pm} = \frac{2}{[(1+n_0)\cos\Theta_{\pm} + i(n_{\pm} + n_0/n_{\pm})\sin\Theta_{\pm}]},$$

and

$$T(B) = \frac{n_0(|t_+|^2 + |t_-|^2)}{2}.$$

Here, the \pm sign refers to the left and right circularly polarized waves, respectively, n_{\pm} is the complex index of refraction and $\Theta_{\pm} = (\omega/c)n_{\pm}z_0$. The thickness of the 2D EG, z_0 , is in the order of 100 \AA , and n_0 is the index of refraction of GaAs. In addition,

$$n_{\pm} = [\epsilon - i\sigma_{\pm}(B)/\omega\epsilon_0]^{1/2},$$

$$\sigma_{\pm}(B) = \frac{n_s e^2}{z_0 m_{CR}^*} \frac{1}{1/\tau_{CR} + i(\omega \pm eB/m_{CR}^*)}.$$

Here, ϵ is the dc dielectric constant, and $\sigma(B)$ is the Drude conductivity at ω in the presence of B .

The transmittance $T(B)$ is calculated using n_s from Eq. (1) and m_{CR}^* given in Fig. 2. The Lorentzian fitting (dashed curves in Fig. 1) was carried out with only one fitting parameter, τ_{CR} . For $V_g \gtrsim -100$ V, the CR line is symmetric and the one parameter fitting is excellent. However, the resonance shows an asymmetric line shape with less absorption in the high B side, when n_s is less than $3 \times 10^{10} \text{ cm}^{-2}$. For example, in the case of $V_g = -150$ V ($n_s = 1.55 \times 10^{10} \text{ cm}^{-2}$), the HWHM are 0.037 and 0.017 T for the low and high B sides, respectively. This makes the determination of τ_{CR} less meaningful. In Fig. 3(a), τ_{CR} extracted from fitting the data is plotted as Γ_{CR} , defined by $\Gamma_{CR} = \hbar/\tau_{CR}$, as a function of V_g , n_s , and ν .

The HWHM of CR will reflect directly the CR mobility μ_{CR} under the condition that the conductivity of the 2D EG at resonance is small enough to be treated as a perturbation. This small absorption approximation is

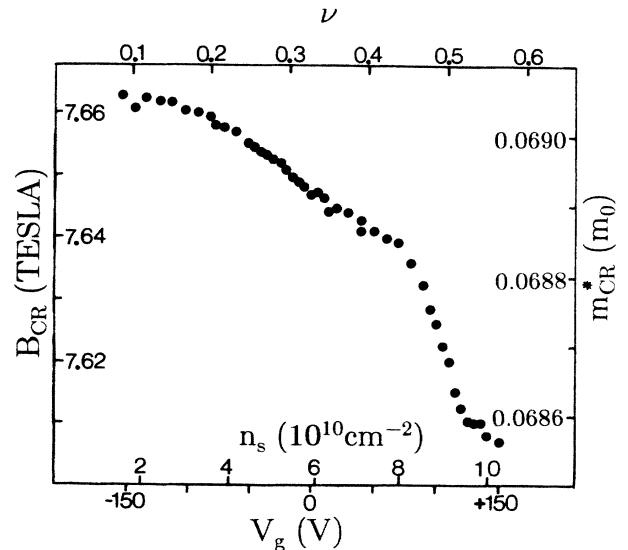


FIG. 2. The cyclotron-resonance position B_{CR} and the corresponding effective mass m_{CR}^* as a function of filling factor ν , carrier density n_s , and back-gate voltage V_g .

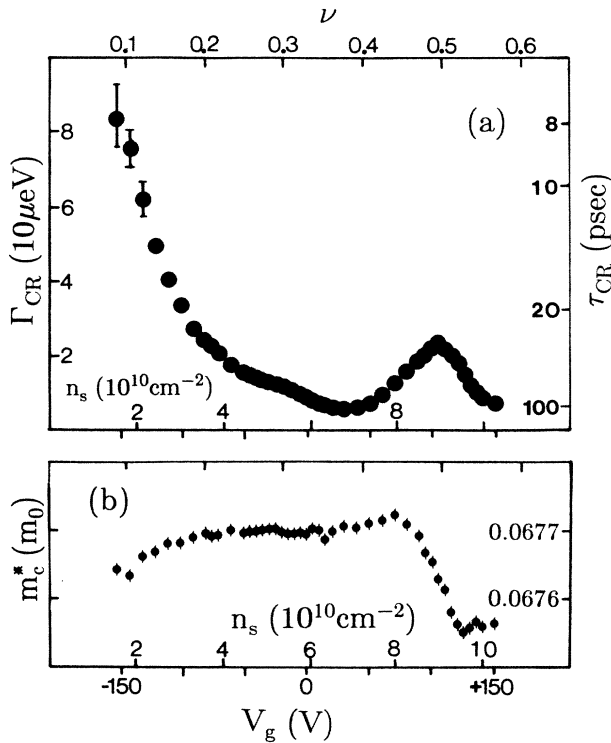


FIG. 3. (a) The fitted CR linewidth and (b) the effective mass after the nonparabolicity correction as a function of ν , n_s , and V_g .

applicable only in the low-mobility regime. For example, for $n_s = 1.0 \times 10^{11} \text{cm}^{-2}$, the transmittance and the absorbance change linearly with respect to μ_{CR} for $\mu_{CR} < 10^5 \text{cm}^2/\text{Vsec}$, and the small absorption approximation is valid. When μ_{CR} is higher, the 2D EG behaves like a metallic sheet and reflects most of the incident FIR. Under such a condition, the transmittance changes sublinearly and the absorbance reaches a maximum and will decrease when μ_{CR} increases further.

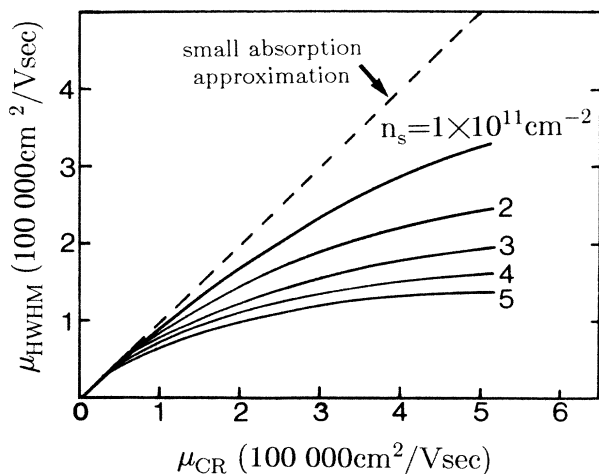


FIG. 4. The effective mobility μ_{HWHM} , obtained from the HWHM of the calculated CR, as a function of the CR mobility with n_s varying from 1×10^{11} to $5 \times 10^{11} \text{cm}^{-2}$.

Thus the mobility obtained from HWHM (μ_{HWHM}) underestimates μ_{CR} and a fitting of the whole CR curve is required to obtain μ_{CR} . This process to extract μ_{CR} is especially required for high-density samples. For example, as shown in Fig. 4, when μ_{CR} changes from 100 000 to 200 000 cm^2/Vsec , μ_{HWHM} changes from 92 000 to 167 000 cm^2/Vsec for $n_s = 1 \times 10^{11} \text{cm}^{-2}$. For $n_s = 5 \times 10^{11} \text{cm}^{-2}$, μ_{HWHM} changes from 66 000 to 99 000 cm^2/Vsec only. For even higher mobilities, the deviation will be much more serious, and eventually, the CR width will not reflect any change of μ_{CR} . This saturation effect is the reason no oscillatory effect in the linewidth has been observed in the high-density samples.⁸

IV. RESULTS AND DISCUSSIONS

A. Level crossing

It is clear from Figs. 3(a) and 2 that Γ_{CR} shows a broad peak near $n_s \sim 9 \times 10^{10} \text{cm}^{-2}$, accompanied by a 0.4% change in m_{CR}^* . Similar broadening accompanied by shift of m_{CR}^* has been observed by several groups,^{15–17} and is attributed to the subband level crossing due to a small angle θ between the normal to the 2D EG and the B direction. If we assume that the measured broadening reflects the level splitting, $\hbar\omega \sin\theta/\sqrt{2}$, the angle θ is estimated to be $\sim 0.3^\circ$. To confirm this level-crossing effect, the sample was tilted intentionally with respect to the B direction. The broadening develops into a well-resolved splitting as the angle θ is increased. The reason that the level crossing occurs at the observed densities is that the subband energies E_i shift relatively closer (farther) to the conduction-band edge at the interface when a positive (negative) back gate bias is applied (here i is the subband index). Our observation indicates that the separation of the lowest two subbands is reduced to 12.85 meV, when $V_g = +105 \text{V}$.

In order to facilitate a quantitative estimation of E_i , we used the triangular approximation,⁴¹ in which the electric field F_s at the interface is assumed constant throughout the space-charge region and the barrier height is assumed infinite. Then, E_i can be obtained as a function of F_s ,

$$E_i(V_g) = \left[\frac{\hbar^2}{2m_c} \right]^{1/3} \left[\frac{3}{2} \pi e F_s(V_g) \right]^{2/3} \left(i + \frac{3}{4} \right)^{2/3},$$

where $F_s(V_g) = F_{s0} - C_{\text{eff}} V_g / e \epsilon \epsilon_0$, F_{s0} is the surface field at zero bias, m_c is the conduction-band-edge mass of GaAs, $m_c = 0.0665 m_0$, and the effective capacitance, C_{eff} , is 46.5 pF/cm², from Eq. (1). From the level-crossing data, $E_1(105 \text{V}) - E_0(105 \text{V}) = \hbar\omega = 12.85 \text{meV}$, and the $E_0(0 \text{V})$, $E_1(0 \text{V})$, and F_{s0} are deduced to be 22 meV, 39 meV, and $1.3 \times 10^6 \text{V/m}$, respectively. This value of F_{s0} corresponds to a total charge, $n_s + N_{\text{dep}}$, of $9.0 \times 10^{10} \text{cm}^{-2}$, where N_{dep} is the total depletion charge in GaAs. Since $n_s = 5.9 \times 10^{10} \text{cm}^{-2}$, $N_{\text{dep}} = 3.1 \times 10^{10} \text{cm}^{-2}$. If we assume that the Fermi level is pinned in the middle of the band gap of the GaAs substrate, and since the depletion length

$$W = \left(\frac{2\epsilon\epsilon_0}{eN_A} \phi_T \right)^{1/2} = N_{\text{dep}}/N_A,$$

and the built-in voltage $\phi_T = 0.79$ eV, the value obtained for N_{dep} implies that $W = 3.7$ μm and the acceptor density $N_A = 8.5 \times 10^{13}$ cm^{-3} .

B. Effective mass

Our results on level crossing demonstrate that E_0 shifts closer (farther) to the conduction-band edge at the interface when a positive (negative) V_g is applied. Since the GaAs conduction band is nonparabolic, m_{CR}^* will decrease with increasing n_s . The effective mass of the conduction-band edge, m_c^* , can be obtained, using the nonparabolicity correction calculated by Ando,⁴²

$$m_c^* = m_{\text{CR}}^* \left\{ 1 + \left[\frac{4}{3} E_0(V_g) + 2\hbar\omega \right] / E_g \right\}^{-1}, \quad (3)$$

where E_g is the band gap of GaAs. The corrected m_c^* is plotted against V_g , n_s , and ν in Fig. 3(b).

The absolute value of m_c^* has an uncertainty of $\sim 1\%$, which is the accuracy of the B field calibration. However, since the resonance is sharp, the relative value of m_c^* is reproducible to better than 0.02% . This extremely high relative accuracy in m_c^* allows us to distinguish the data in three different regions. In the region $0.4 < \nu < 0.6$, the effect of level crossing dominates m_c^* as well as Γ_{CR} . Since the second Landau level of the ground subband is perturbed by the first Landau level of the first excited subband, and m_c^* measures the average separation of the first two Landau levels of the ground subband, it is expected that m_c^* reflects this perturbation. In Fig. 3(b), m_c^* shows first a slight increase at $\nu \gtrsim 0.4$ and then a 0.27% decrease at $\nu \sim 0.5$, consistent with the fact that the subband separation E_{10} decreases as V_g becomes more positive. In the region from $\nu \simeq 0.4$ to $\nu \simeq 0.14$, m_c^* is constant to better than 0.025% . This constancy in m_c^* over an n_s range from 7×10^{10} to 3×10^{10} cm^{-2} should be contrasted to the results from previous experiments on Si inversion layers,³⁻⁵ where electron localization, evident from the thermally activated conduction, occurs in the low- n_s regime.⁴³ Localization causes the CR effective mass to shift to lower values, and leads to an asymmetric line shape. Our result that m_c^* is constant may be regarded as an indication that the 2D electrons are not localized even at a density as low as 3.0×10^{10} cm^{-2} . As n_s is further decreased, m_c^* is slightly reduced and an asymmetric line shape is observed. This observation suggests that localization may start to influence the resonance position and the line shape.

C. Level broadening

The CR linewidth is extremely narrow near $\nu \simeq 0.4$. The τ_{CR} (or Γ_{CR}) obtained from fitting the resonance line shape is 104 ps (or 6.3 μeV) at $n_s \simeq 7 \times 10^{10}$ cm^{-2} , which is 15 times longer than that obtained from μ_{dc} ($\tau_{\text{dc}} \simeq 7$ ps).

This narrow linewidth prompts us to reexamine the dominant broadening mechanism of Landau levels. Generally speaking, the broadening can be divided into two categories, inhomogeneous and homogeneous (or lifetime) broadenings. If the Landau-level width is determined by the inhomogeneous broadening, Γ_{CR} is proportional to the difference of the two levels, i.e., $\Gamma_{\text{CR}} \sim \Gamma_0 - \Gamma_1$, where Γ_0 and Γ_1 are the half-width of the first and second Landau levels, respectively. For lifetime broadening, Γ_{CR} , on the other hand, is the sum of Γ_0 and Γ_1 . Consequently, Γ_{CR} is expected to satisfy the relation, $\Gamma_0 - \Gamma_1 < \Gamma_{\text{CR}} < \Gamma_0 + \Gamma_1$, under the circumstance that both inhomogeneous and lifetime broadening contribute, and both should be included. In a 2D system, the inhomogeneous broadening is due to long-range potential fluctuations, e.g., the unscreened Coulomb potential of an ionized impurity. However, a long-range potential can cause both inhomogeneous and lifetime broadenings. Of importance is the ratio of the potential range d to l_0 . If $2d < l_0$, lifetime broadening dominates the Landau-level broadening. On the other hand, if $d > l_0$, the inhomogeneous broadening will be dominant.^{23,24} We should find out the dominant scatterers in our sample in the extreme quantum limit, and its potential range.

In principle, there are different scattering processes going on at the same time, e.g., electrons can be scattered by impurities (elastic scattering), acoustic phonons and electrons themselves (inelastic scatterings), and the

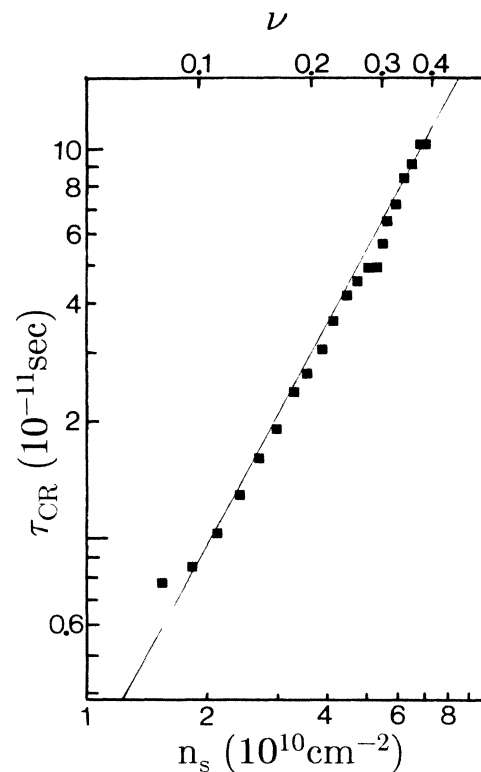


FIG. 5. The fitted CR lifetime as a function of n_s and ν . The straight line is a guide for the eye, indicating $\tau_{\text{CR}} \propto n_s^{1.9}$.

level width due to lifetime broadening is the sum of the broadening due to each type of scattering separately. The acoustic-phonon scattering time τ_{ac} and the electron-electron scattering time, τ_{e-e} have been studied thoroughly in the absence of B .⁴⁴ In the presence of B , not only does the density of states become discrete, also the electron wave function is different. It is expected that both τ_{ac} and τ_{e-e} are radically altered, and are longer due to the requirements of conservation of energy and angular momentum. In our data, the τ_{CR} decreases strongly as n_s is decreased, excluding the possibility that the level broadening is dominated by either $1/\tau_{ac}$ or $1/\tau_{e-e}$. In fact, as shown in Fig. 5, the τ_{CR} depends on n_s following a power law $\tau_{CR} \propto n_s^{1.9 \pm 0.1}$ in the n_s range $2.1 \times 10^{10} < n_s < 7.0 \times 10^{10} \text{ cm}^{-2}$, when the ionized impurity scattering is believed to be the dominant broadening mechanism.

The level broadening due to impurity scattering has been investigated self-consistently by several groups.²⁵⁻²⁸ Das Sarma²⁵ pointed out that the screening of ionized impurities by electrons depends strongly on the density of states at E_f and leads to the oscillation of Γ_{CR} as a function of ν . Ando²⁸ showed that, at $\nu=0.5$, screening is so strong that any remote ionized impurities, e.g., Si donors, have hardly any influence on Γ_0 . Consequently, Γ_0 and Γ_{CR} are determined by the concentration of residual acceptors, N_A , in GaAs. Since our setback thickness is 910 Å, too far to affect Γ_0 , the observed Γ_{CR} of 6.3 μ eV at $\nu \sim 0.4$ should give the N_A in GaAs. We compared the Γ_{CR} in Fig. 3 with the calculations of Ref. 28, and obtained $N_A \lesssim 1.0 \times 10^{14} \text{ cm}^{-3}$, which is in good agreement with that obtained from the level-crossing effect. Since screening is expected to be strong at $\nu \sim 0.4$, the range of the acceptor potential is substantially reduced, in contrast to the case in the absence of B . As a result, the dc scattering time τ_{dc} is expected to be much shorter than τ_{CR} , assuming that the dominant scatterers are the same. Indeed, the τ_{dc} is 15 times shorter than τ_{CR} , for $n_s = 6.8 \times 10^{10} \text{ cm}^{-2}$. When n_s is decreased, the screening ability becomes weaker, which increases the range of the repulsive potential of the acceptors and the scattering probability $1/\tau_{CR}$. The observation that $\tau_{CR} \propto n_s^{1.9 \pm 0.1}$ down to $\nu=0.12$ implies that the screened electron-acceptor scattering dominates the broadening of Landau levels in the range $0.12 \leq \nu \leq 0.4$. As pointed out by Ando,^{21,27} when the repulsive impurity concentration is low and the range of potential is short, the inhomogeneous broadening can be ignored. That is to say, the distribution of density of states should be symmetric, a consequence of lifetime broadening, and this is the sufficient condition for the observed symmetric line shape in the range $0.17 < \nu < 0.4$. The ob-

served asymmetric line shape at low ν ranging from $0.085 \leq \nu \leq 0.17$ may result from inhomogeneous broadening, as discussed previously. When ν decreases, the screening ability becomes weaker and any attractive potential (other than acceptor potential) with range $d \gtrsim l_0$ can localize electrons, and give rise to an asymmetric distribution of density of states. Thus the CR absorption from different regions of the sample gives rise to an asymmetric line shape. On the other hand, the importance of electron correlation has long been anticipated.^{6,7} It is unclear at present if the asymmetry and line shift may also result from correlation effects.

V. CONCLUSION

We have demonstrated the existence of a high-mobility 2D EG at low densities down to $n_s = 1.55 \times 10^{10} \text{ cm}^{-2}$. By choosing a short FIR wavelength of 96.52 μm, the CR is studied in the extreme quantum limit, $0.086 \leq \nu \leq 0.57$. In the range $0.4 < \nu \leq 0.57$, the subband level crossing dominates the line broadening and the line shift. The lowest subband and the first excited subband energies are estimated from a study of the level crossing to be 22 and 39 meV, respectively. In addition, the total depletion charge and the residual acceptor density in GaAs are deduced to be $3.1 \times 10^{10} \text{ cm}^{-2}$ and $8.5 \times 10^{13} \text{ cm}^{-3}$. When the lowest Landau level is close to half filled, $\nu \sim 0.4$, the extracted τ_{CR} is 104 ps, the longest reported to date. This long lifetime makes it possible for us to determine the acceptor density in GaAs to be $N_A \lesssim 1.0 \times 10^{14} \text{ cm}^{-3}$, consistent with that obtained from the level-crossing effect. In the range $0.12 < \nu < 0.4$, τ_{CR} decreases with decreasing n_s following $\tau_{CR} \propto n_s^{1.9 \pm 0.1}$. We attribute this n_s -dependent τ_{CR} in the extreme quantum limit to scattering by the screened residual ionized impurities in GaAs.

Finally, it is known that a 2D EG with a relatively low amount of disorder forms fractional quantum Hall (FQH) states at odd-denominator fractional fillings. We have extended our study of CR to $T = 2.3 \text{ K}$, and examined the linewidth of the CR and found no structures at $\nu = \frac{1}{3}, \frac{1}{5}$, and $\frac{1}{11}$. This result is consistent with Kohn's theorem⁴⁵ that in a translationally invariant system, the electron-electron interaction effects cannot influence the resonance position. However, our experiment is carried out at relatively high T and a low- T experiment is currently under way to study the CR of electrons in the FQH states.

ACKNOWLEDGMENTS

This work is supported in part by the U.S. Air Force Office of Scientific Research and by the U.S. Office of Naval Research.

¹G. Abstreiter, P. Kneschaurek, J. P. Kotthaus, and J. F. Koch, Phys. Rev. Lett. **32**, 104 (1974).

²S. J. Allen, Jr., D. C. Tsui, and J. V. Dalton, Phys. Rev. Lett. **32**, 107 (1974).

³J. P. Kotthaus, G. Abstreiter, J. F. Koch, and R. Ranvaud,

Phys. Rev. Lett. **34**, 151 (1974).

⁴H. Kublbeck and J. P. Kottaus, Phys. Rev. Lett. **35**, 1019 (1975).

⁵T. A. Kennedy, R. J. Wagner, B. D. McCombe, and D. C. Tsui, Solid State Commun. **21**, 459 (1977).

- ⁶S. J. Allen, Jr., B. A. Wilson, and D. C. Tsui, *Phys. Rev. B* **26**, 5590 (1982).
- ⁷Z. Schlesinger, W. I. Wang, and A. H. MacDonald, *Phys. Rev. Lett.* **58**, 73 (1987).
- ⁸Th. Englert, J. C. Maan, Ch. Uihlein, D. C. Tsui, and A. C. Gossard, *Solid State Commun.* **44**, 1301 (1982).
- ⁹Z. Schlesinger, S. J. Allen, Jr., J. C. M. Hwang, P. M. Platzman, and N. Tzoar, *Phys. Rev. B* **30**, 435 (1984).
- ¹⁰B. A. Wilson, S. J. Allen, Jr., and D. C. Tsui, *Phys. Rev. Lett.* **44**, 479 (1980).
- ¹¹M. A. Brummell, R. J. Nicholas, L. C. Brunel, S. Huant, M. Baj, J. C. Portal, M. Razeghi, M. A. di Forte-Poisson, K. Y. Cheng, and A. Y. Cho, *Surf. Sci.* **142**, 380 (1984).
- ¹²K. Muro, S. Mori, S. Narita, S. Hiyamizu, and K. Nanbu, *Surf. Sci.* **142**, 394 (1984).
- ¹³D. Heitmann, M. Ziesmann, and L. L. Chang, *Phys. Rev. B* **34**, 7463 (1986).
- ¹⁴M. J. Chou and D. C. Tsui, *MRS Symp. Proc.* **37**, 7 (1985).
- ¹⁵Z. Schlesinger, J. C. M. Hwang, and S. J. Allen, Jr., *Phys. Rev. Lett.* **50**, 2098 (1983).
- ¹⁶G. L. J. A. Rikken, H. Sigg, C. J. G. M. Langerak, H. W. Myron, J. A. A. J. Perenboom, and G. Wiemann, *Phys. Rev. B* **34**, 5590 (1986).
- ¹⁷A. D. Wieck, J. C. Maan, K. Ploog, U. Merkt, and J. P. Kotthaus, in *Proceedings of the 18th International Conference on Physics of Semiconductors, City, 1986* (unpublished).
- ¹⁸G. Abstreiter, J. P. Kotthaus, J. F. Koch, and G. Dorda, *Phys. Rev. B* **14**, 2480 (1976).
- ¹⁹P. Voisin, Y. Guldner, J. P. Vieren, M. Voos, P. Delescluse, and N. T. Linh, *Appl. Phys. Lett.* **39**, 982 (1981).
- ²⁰H. J. Mikeka and H. Schmidt, *Z. Phys. B* **20**, 43 (1975).
- ²¹T. Ando, *J. Phys. Soc. Jpn.* **38**, 989 (1975).
- ²²C. S. Ting, S. C. Ying, and J. J. Quinn, *Phys. Rev. Lett.* **37**, 215 (1976).
- ²³M. Prasad and S. Fujita, *Physica* **91A**, 1 (1978).
- ²⁴W. Gotze and J. Hajdu, *Solid State Commun.* **29**, 89 (1979).
- ²⁵S. Das Sarma, *Phys. Rev. B* **23**, 4592 (1981).
- ²⁶R. Lassing and E. Gornik, *Solid State Commun.* **47**, 959 (1983).
- ²⁷T. Ando, *J. Phys. Soc. Jpn.* **52**, 1740 (1983); **53**, 3101 (1984); **53**, 3126 (1984).
- ²⁸T. Ando, *J. Phys. Soc. Jpn.* **54**, 1519 (1985).
- ²⁹A. Gold, *Z. Phys. B* **63**, 1 (1986).
- ³⁰C. Kallin and B. I. Halperin, *Phys. Rev. B* **31**, 3635 (1985).
- ³¹W. G. Keppmann and R. J. Elliott, *J. Phys. C* **8**, 2729 (1975).
- ³²D. C. Tsui, H. L. Stormer, and A. C. Gossard, *Phys. Rev. Lett.* **48**, 1562 (1981).
- ³³R. B. Laughlin, *Phys. Rev. Lett.* **50**, 1395 (1983).
- ³⁴See, e.g., T. Ando, A. B. Fowler, and F. Stern, *Rev. Mod. Phys.* **54**, 516 (1982).
- ³⁵H. L. Stormer, R. Dingle, A. C. Gossard, W. Wiegmann, and M. D. Sturge, *Solid State Commun.* **29**, 705 (1979).
- ³⁶J. H. English, A. C. Gossard, H. L. Stormer, and K. W. Baldwin, *Appl. Phys. Lett.* **50**, 1826 (1987).
- ³⁷H. L. Stormer, A. C. Gossard, W. Wiegmann, and K. Baldwin, *Appl. Phys. Lett.* **39**, 912 (1981).
- ³⁸M. Chou, D. C. Tsui, and G. Weimann (unpublished).
- ³⁹D. C. Tsui, A. C. Gossard, G. Kaminsky, and W. Wiegmann, *Appl. Phys. Lett.* **39**, 712 (1981).
- ⁴⁰T. Ando, *J. Phys. Soc. Jpn.* **51**, 3900 (1982).
- ⁴¹F. Stern, *Phys. Rev. B* **5**, 4891 (1972).
- ⁴²T. Ando, *J. Phys. Soc. Jpn.* **51**, 3893 (1982).
- ⁴³D. C. Tsui and S. J. Allen, Jr., *Phys. Rev. Lett.* **32**, 1200 (1974); S. J. Allen, Jr. and D. C. Tsui, *ibid.* **35**, 1359 (1975).
- ⁴⁴E. M. Conwell, *High Field Transport in Semiconductors* (Academic, New York, 1967), Chap. 3.
- ⁴⁵W. Kohn, *Phys. Rev.* **123**, 1242 (1961).